

Scientific Report within the ESF activity “New Generation of Organic Based Photovoltaic Devices”

Applicant:

Evren Aslan Gürel

Department of Chemistry and Biochemistry

University Berne

Freiestrasse 3

3012 Bern, Switzerland

evren.aslan@iac.unibe.ch

Hosting group:

Prof.Dr.N. Serdar Sariciftci

Linz Institute for Organic Solar Cells

Institute of Physical Chemistry

Johannes Kepler University of Linz

Altenbergerstr. 69

A 4040 Linz, Austria

serdar.sariciftci@jku.at

Preparation and Characterization of Nanostructured Hybrid Solar Cells

Objectives :

The position of the conduction and valence bands of semiconductor quantum dots is determined by the material and also the size of the quantum dots. In this study, processes are investigated for the fabrication of hybrid bilayer photovoltaic (PV) devices consisting of semiconductor quantum dots (NCs) having different sizes and a conjugated polymer. Our design utilizes that a large band gap Titanium dioxide (TiO_2) and an organic p-type material poly [2-methyl, 5-(3,7** dimethyl-octyloxy)-p- para-phenylene vinylene) (MDMO-PPV) was sensitized to visible light using Cadmium Telluride (CdTe) quantum dots. CdTe quantum dots layer was formed with self-assembly technique on mercaptopropionic acid (MPA)/ TiO_2 /ITO surface. Solar cells were then produced by spin coating of (MDMO-PPV) and evaporation of gold as the back contact. Optical, electrical and morphological properties of this novel prototype of solar cells were investigated. CdTe nanocrystals are demonstrated to increase the photon-harvesting efficiency of hybrid solar cells.*

In the second part, a solid state solar cell using a nanocrystalline TiO_2 film electrode modified by Cu-chlorophyllin coppered (CHPL) and poly-3-hexylthiophene (P3HT) was developed. CHPL is a cheaper alternative to Ru dyes. CHPL and P3HT were used as dye and hole transport material, respectively. Atomic force microscope (AFM) analysis reveals that the TiO_2 film is composed of interconnected particles and pores. Sensitization of electrode with CuChl molecules extends the absorbance of the electrode into the visible region. For a cell using CuChl and P3HT adsorbed on a nanocrystalline TiO_2 film electrode, I_{SC} , V_{OC} and FF were 0.42 mA cm^{-2} , 300 mV, and 32%, respectively.

Work carried out during the visit

PART 1:

1.1 Experimental

Spectroscopic analyses were carried out using stable dispersions. Absorption spectra were recorded on a Varian Carry spectrophotometer. Fluorescence spectra were taken with Carry Eclipse Fluorescence Spectrophotometer. Atomic force microscope (AFM) measurements were done with a Dimension 3100 instrument from Digital Instrument (Santa Barbara, CA) in tapping mode. AFM pictures were applied to check the roughness of the films.

All current–voltage (I–V) characteristics of the PV devices were measured (using a Keithley SMU 236) in a glove box immediately after production. A Steuernagel solar simulator, simulating AM1.5 conditions, was used as the excitation source with an input power of 100 mW/cm² white-light illumination. The photovoltaic power conversion efficiency of a solar cell is determined by the following formula:

$$\eta_e = \frac{V_{oc} * I_{sc} * FF}{P_{in}}$$

Equation 1

$$FF = \frac{I_{mpp} * V_{mpp}}{I_{sc} * V_{oc}}$$

Equation 2

where V_{oc} is the open circuit voltage, I_{sc} is the short circuit current, FF is the fill factor and P_{in} is the incident light power density, I_{mpp} and V_{mpp} are the current and voltage at the maximum power point in the fourth quadrant of the current-voltage characteristics.

The spectrally resolved photocurrent was measured with a EG&G Instruments 7260 lock-in amplifier. The samples were illuminated with monochromatic light from a Xenon lamp. The incident photon to current efficiency (% IPCE) was calculated according to the following equation:

$$\text{IPCE (\%)} = \frac{I_{sc} * 1240}{P_{in} * \lambda_{incident}}$$

Equation 3

where I_{sc} ($\mu\text{A}/\text{cm}^2$) is the measured current under short-circuit conditions of the solar cell, P_{in} (W/m^2) is the incident light power, measured with a calibrated silicon diode, and λ (nm) is the incident photon wavelength¹.

1.2 Assembling Procedure

Ti-Nanoxide T/SC (Solaronix) (5% v/v in ethanol) was drop casted on cleaned ITO glass. These TiO_2 were sintered in ambient conditions at 450 °C for 1h. Typical film thickness of the TiO_2 film, measured from the cross sectional image of an Atomic Force Microscopy (AFM), was about 1.5 μm . From previous reports, the thicker TiO_2 films (more than 2 μm) did not exhibit any good effects on the photocurrent and overall efficiency in CdSe sensitized cells².

The poor performance of the QD-SSCs may be ascribed to the difficulty of assembling the QDs into the mesoporous TiO_2 matrix to obtain a well-covered QD layer on the TiO_2 crystalline surface³. In the literature, attachment of CdSe QDs to nanocrystalline TiO_2 has been shown to be successful with an immersion method using a bimolecular linker⁴. Here, mercaptopropionic acid (MPA) was used as linker and all prepared TiO_2 electrodes were exposed to MPA (5mM, in ethanol) for 15h. QDs were adsorbed to modified ITO/ TiO_2 /MPA for 1h and afterwards these QDs modified electrodes washed and dried in air. For multilayer QD solar cells, MPA stabilized CdTe quantum dots sequentially layered with poly(diallyldimethylammonium chloride)(5% w/v in water) polyelectrolyte (Figure 1.1) .

PDADMAC [poly\(diallyldimethylammonium chloride\)](#) is a synthetic homopolymer of diallyldimethylammonium chloride, a poly(quaternary ammonium) and charged all over pH range. PDADMAC with $M_w \approx 10\text{-}20 \times 10^4 \text{ g mol}^{-1}$, 40 % (wt/wt) in water, was purchased from Sigma- Aldrich.

Rainbow type solar cells: ITO/ TiO_2 /MPA/(CdTe_{1.91nm}-PDADMAC)/(CdTe_{1.83nm}-PDADMAC)//(CdTe_{1.74nm}-PDADMAC)/MDMO-PPV/Au

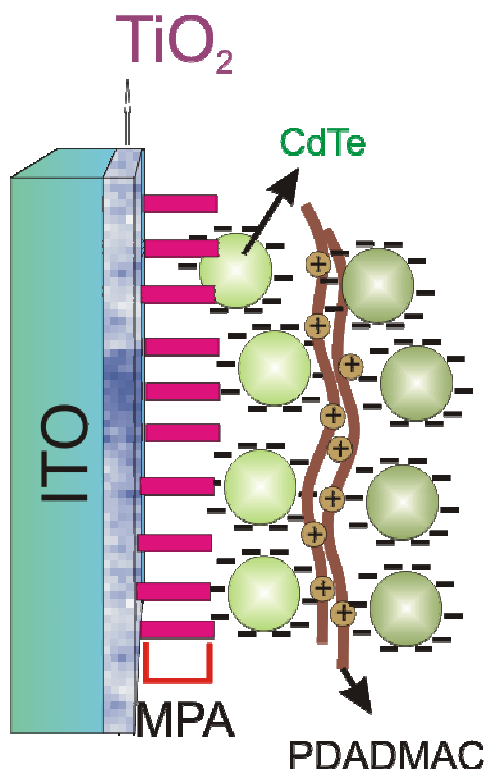


Figure 1.1. Schematic representation of multilayer structure used in solar cells

[MDMO-PPV, poly\[2-methyl, 5-\(3*,7** dimethyl-octyloxy\)-p- para-phenylene vinylene\]](#) (Mw 1.150.000 g/mol) (Covion) is one of the most widely investigated polymer for solar cell purposes. It does usually act as electron donating (p-type) material (Figure 1.2). (%1 wt/wt, in chlorobenzene) solution of MDMO-PPV was spincoated on (ITO/TiO₂/MPA/CdTe) modified electrodes.

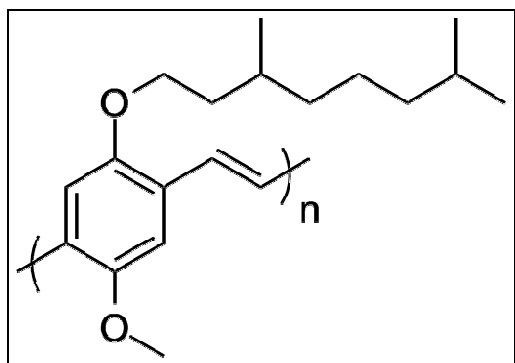


Figure 1.2. Chemical structure of poly[2-methyl, 5-(3*,7** dimethyl-octyloxy)-p- para-phenylene vinylene] (MDMO-PPV)

Finally, Au was evaporated as back contact (100 nm thickness). The device structure of studied solar cells is shown in Figure 1.3.

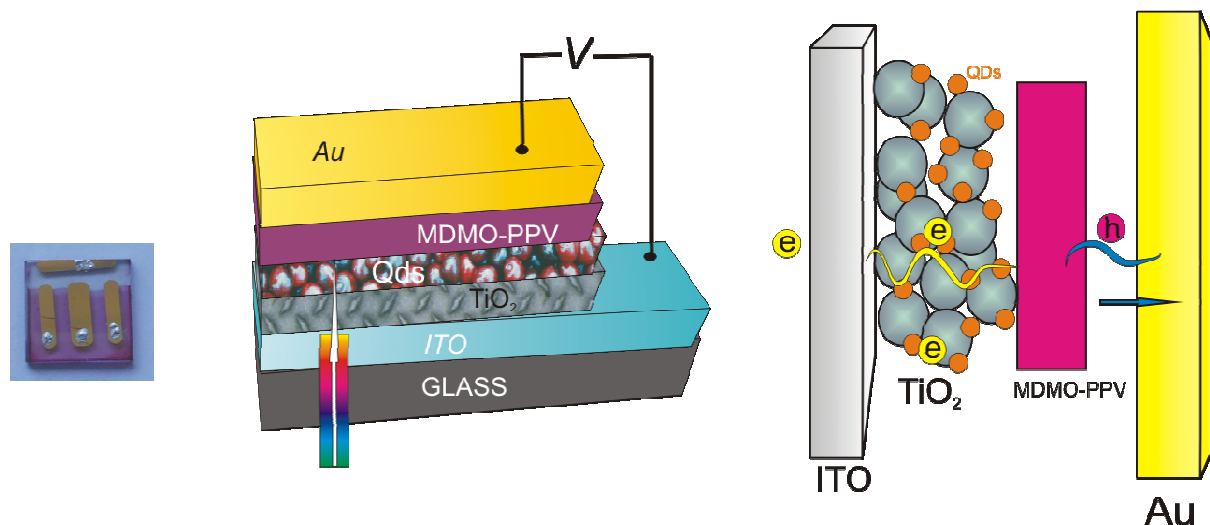


Figure 1.3. Device structure of studied solar cells

Results

1.3 UV-vis Absorption Spectra

The absorption spectra of CdTe QDs prepared with different sizes exhibited the characteristic sharp peaks at their band edges (Figure 1.4), and their sizes were estimated to be about 1.74 nm (460 nm), 1.83 nm (480 nm) and 1.91 nm (500 nm), respectively (Table 1).

Table 1 Size Obtained absorption maxima (λ_{\max}) and optical band gap energies (E_{BG}) for several synthesis times and corresponding radii (R) of CdTe

Sample	t_{synth} (min)	λ_{\max} (nm)	E_{BG} (eV)	R (nm)
CdTe	1	460	2.33	1.74
CdTe	30	480	2.25	1.83
CdTe	200	500	1.85	1.91

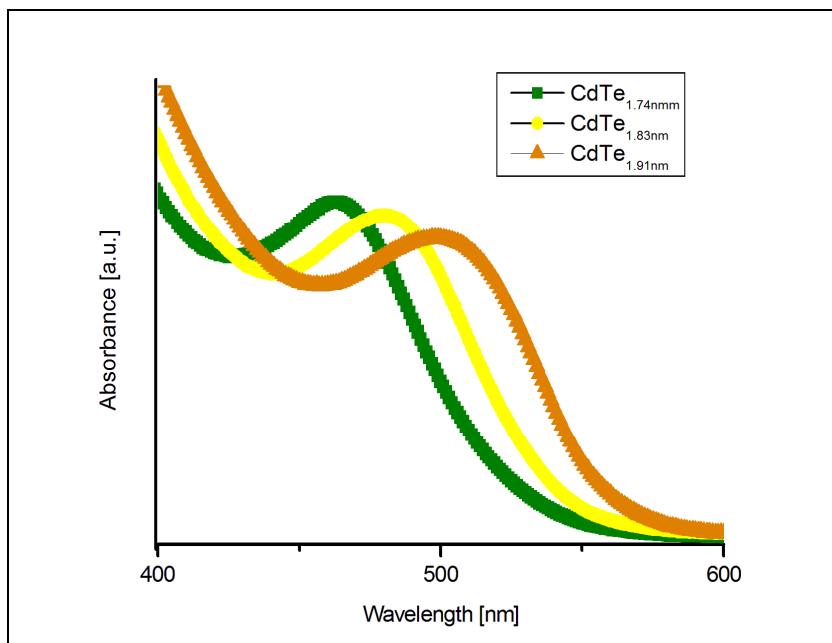


Figure 1.4 UV-Vis absorption spectra of CdTe QDs

The photoluminescence (PL) spectrum of (CdTe-MPA-TiO₂-ITO) electrode is shown in Figure 1.5.a, which is practically identical to the one obtained in solution except for the scattering effects from TiO₂ layers. These observations manifest that the two step procedure is effective in anchoring the dispersed CdTe QDs onto the TiO₂ layer. In previous studies by Nozik *et al*, InP and InAs QDs surrounded with TOPO were observed to be attached well over mesoporous TiO₂ layers without using linker molecules. However, in other reports, the bifunctional linker molecules such as MPA seemed to be essential in anchoring QDs efficiently⁴⁻⁶. For example, a similar procedure was used to link CdSe QDs with TiO₂ using MPA by the Kamat's group recently⁷. In another report, the effect of linker molecules such as 4-mercaptobenzoic acid, 2,3- dimercaptosuccinic acid and mercaptopropionic acid (MPA) was investigated and the best and the most reproducible data were obtained when using MPA, which anchors the QDs onto the TiO₂ surface⁸. In our case, when CdTe QDs were anchored onto (ITO/TiO₂ /MPA) surface, the surface has the same color of QDs (Figure 1.5.b) .

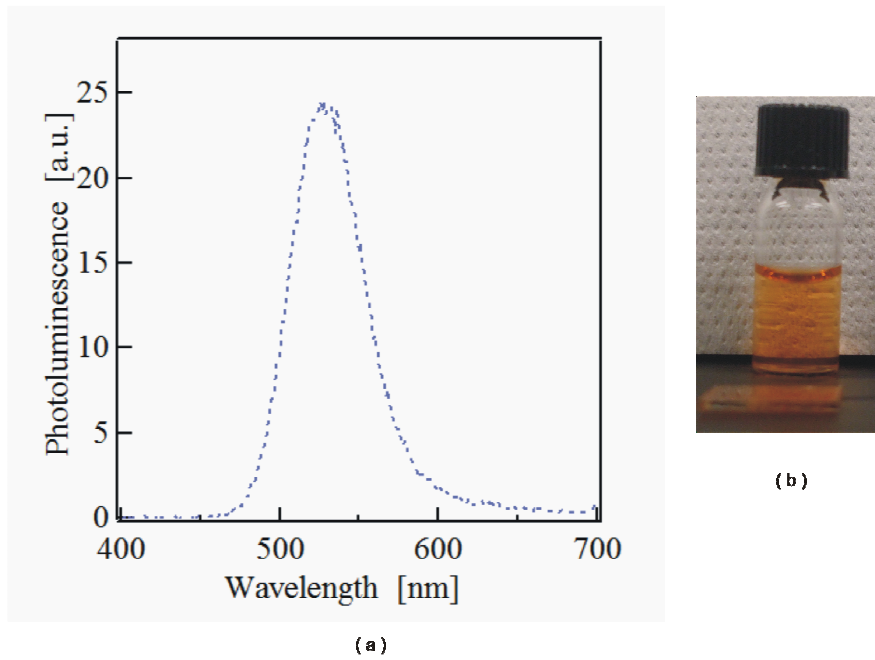


Figure 1.5 (a) Photoluminescence spectrum of ITO/TiO₂/CdTe electrode (b) CdTe QD solution and the picture of ITO/TiO₂/CdTe surface

1.4 AFM study of surfaces

The challenge in solar cells is to organize donor and acceptor materials in a nanometer scale⁹. To correlate the morphology of the solar cells to the photovoltaic performance, AFM measurements were performed. Figure 1.6 shows the AFM images of samples ITO-TiO₂ and ITO-TiO₂-CdTe (1.91nm). Particles are distributed all over the TiO₂ surface and the Q-dots do not introduce changes in the topography of the TiO₂ film.

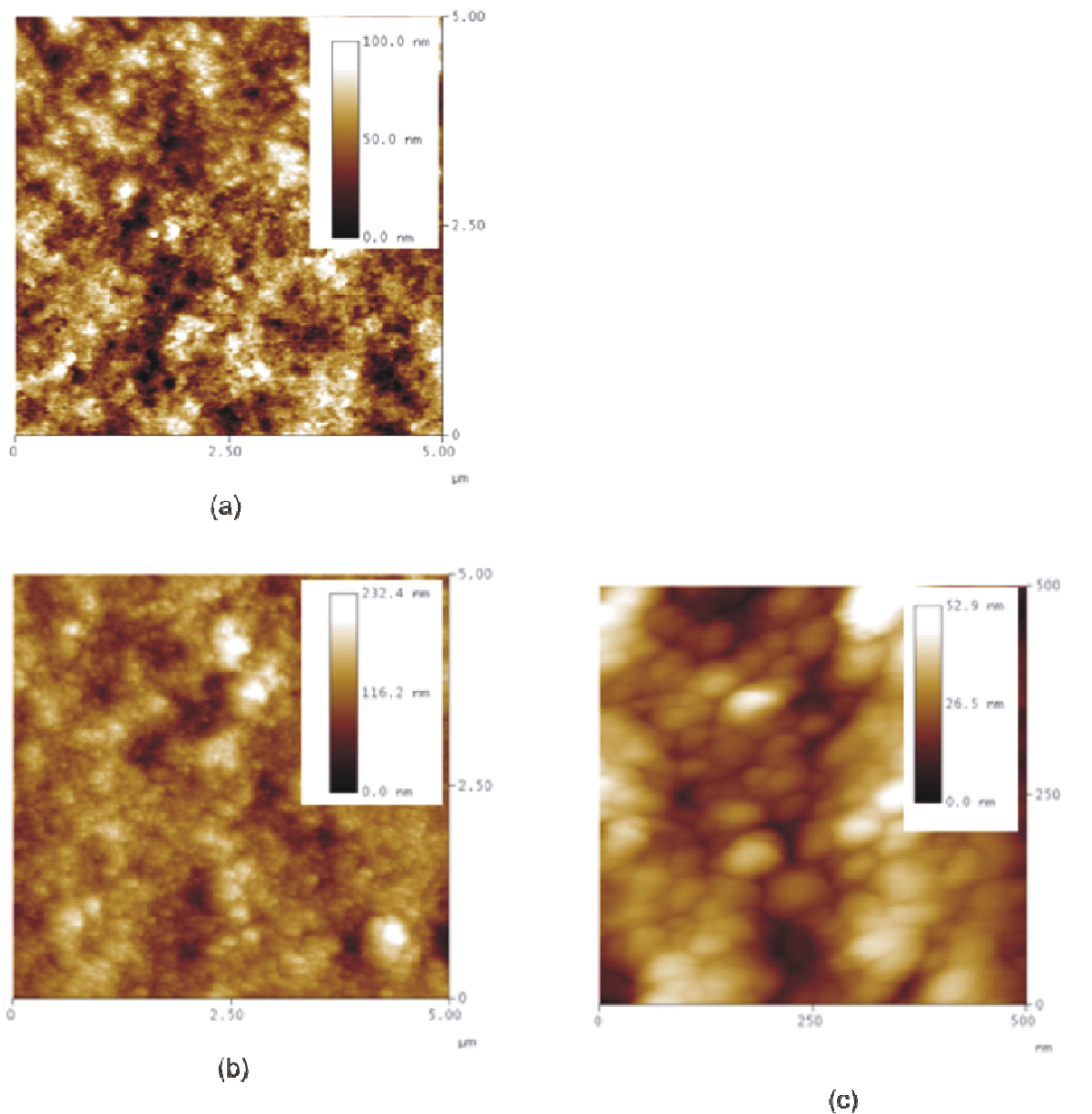


Figure 1.6. AFM images showing the surface morphology of (a) ITO-TiO₂ and (b)-(c) ITO- TiO₂- CdTe(1.91nm)

1.5 Incident Photon to Current Efficiency of Solar Cells

The percent IPCE is the percentage of electrons, measured under short-circuit current conditions, that are related to the number of incident photons, and is used to obtain information on the number of photons of different energy that contribute to charge generation in the solar cell. The reference sample ITO/TiO₂/MPA/MDMO-PPV/Au (without QDs) shows a photoresponse lower than CdTe sensitized solar cells. The spectral response (IPCE) for the different sizes of CdTe QDs solar cells are shown in Figure 1.7.

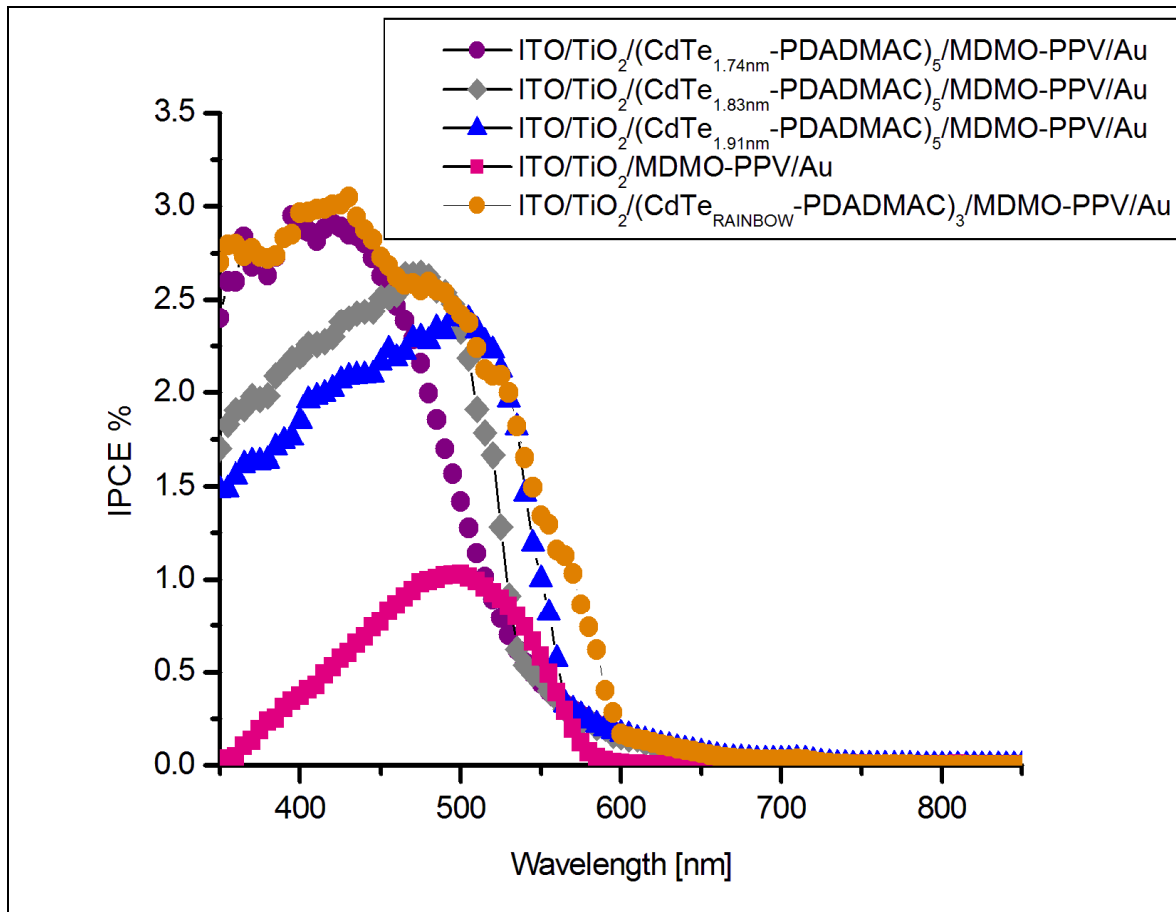


Figure 1.7 IPCE spectra for photovoltaic devices using (CdTe-PDADMAC) multilayers

Compared to the reference sample (ITO/TiO₂/MPA/MDMO-PPV/Au), the multilayer samples show an increase in the spectral range between 400 and 550nm, indicating that the QDs is effectively absorb the light and transfer the charge between the layers. IPCE maximums of all samples in the spectral range from 420 and 510 show ca. 6 times larger ordinate scaling compared to reference sample. From the low IPCE values in the visible region, it seems that some extra energy is necessary to make an efficient charge transfer between TiO₂ and QDs as well as QDs and MDMO-PPV.

The rainbow solar cells employ an ordered assembly of CdTe nanoparticles of different diameters. As white light enters the cell, smaller sized (larger band gap) CdTe particles absorb the portion of the light with smaller wavelengths (blue region). Light with longer wavelengths (red region), which is transmitted through the initial layer, is absorbed by subsequent layers, and so on. By creating an orderly gradient of quantum dots of different size, it should be possible to increase the effective capture of incident light. A rainbow cell configuration allows one to couple the faster electron injection rate of small-sized particles and greater absorption range of large particles effectively.

According to Kamat's *etal* ⁷, in terms of the electron injection rate from CdSe QDs to the TiO₂ conduction band, it was reported to be dependent on the size of CdSe QDs and appeared accelerated for smaller sizes of CdSe QDs.

1.6 Current-Voltage characteristics of devices featuring CdS and CdTe sensitized TiO₂ mesoporous films and MPMO-PPV Polymers

The photovoltaic properties of the solar cells were characterized by measuring current–voltage (*I–V*) curves in the dark and under simulated white-light illumination (AM1.5, 100 mWcm⁻²; AM: air mass) through the ITO side. Figure 1.8 shows the *I–V* characteristics of the heterojunctions prepared with different sized CdTe – MDMO-PPV polymer. Incorporation of the CdTe quantum dots improves the rectification of the diodes, proving the high photosensitivity of the solar cells. For CdTe_{1.74nm}, values of V_{oc} =300 mV, J_{sc} =0.46 mAcm⁻², and a fill factor of 0.25, for CdTe_{1.83nm}, values of V_{oc} =300 mV, J_{sc} =0.36 mAcm⁻², and a fill factor of 0.26 and for CdTe_{1.91nm}, values of V_{oc} =300 mV, J_{sc} =0.34 mAcm⁻², and a fill factor of 0.30 were obtained (Table 2).

Electrostatic adsorption of CdTe generates an ultrathin film with higher light capture cross section. CdTe allow to absorb more light and increase the open circuit voltage without affecting the transport properties (as monitored by the FF) in a substantial manner.

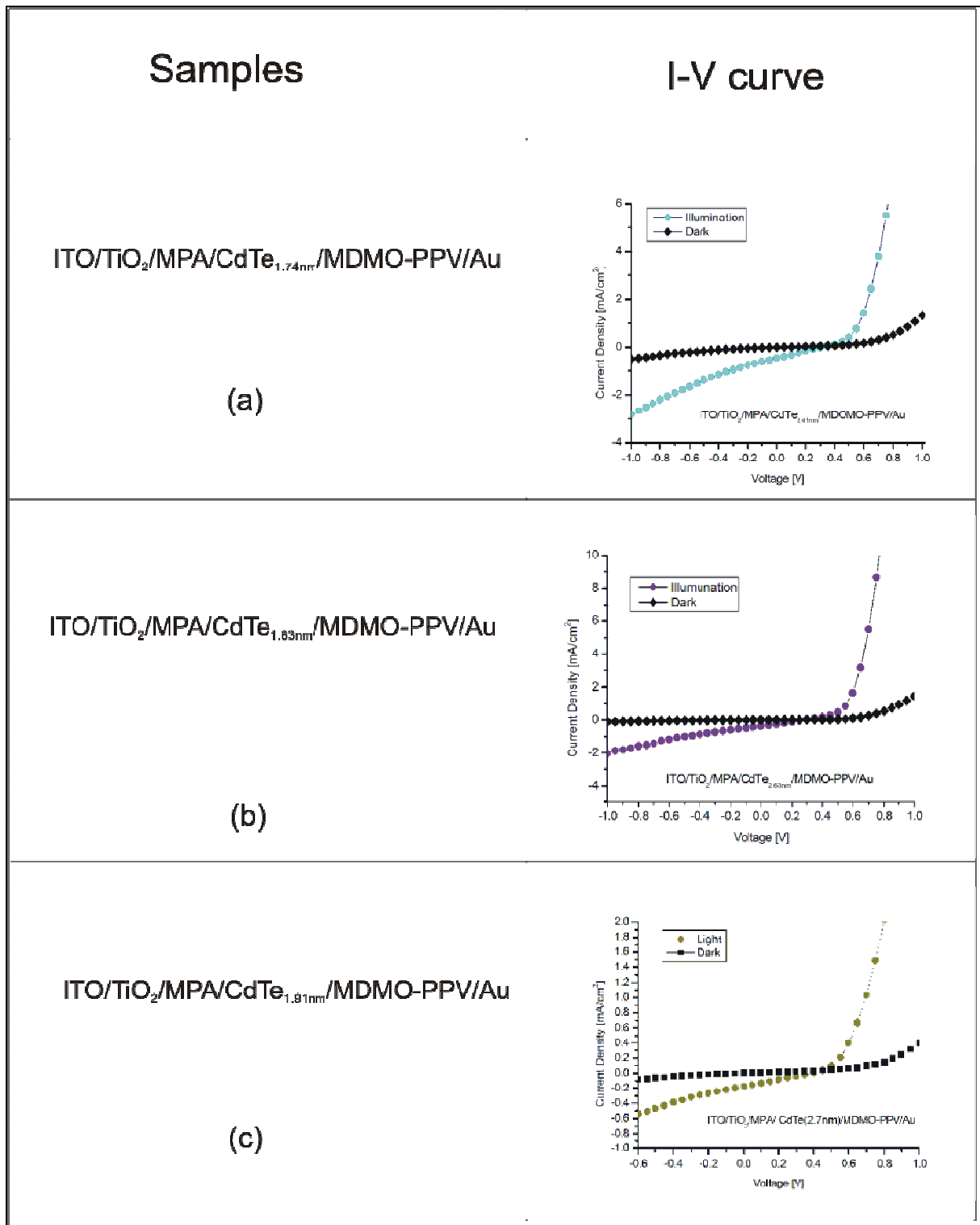


Figure 1.8 Current density vs Voltage(J-V) characteristics of solar cells with the structure of (a) ITO/TiO₂/MPA/CdTe_{1.74nm}/MDMO-PPV/Au (b) ITO/TiO₂/MPA/CdTe_{1.83nm}/MDMO-PPV/Au (c) ITO/TiO₂/MPA/CdTe_{1.91nm}/MDMO-PPV/Au

Table 2 Characteristics of the QDs sensitized solar cells

Sample	J_{sc} (mA/cm ²)	V_{oc} (mV)	FF	MP(μW)
ITO/TiO ₂ /MPA/CdTe _{1.74nm} /MDMO-PPV/Au	0.46	300	0.252	4.3
ITO/TiO ₂ /MPA/CdTe _{1.83nm} /MDMO-PPV/Au	0.36	300	0.261	3.6
ITO/TiO ₂ /MPA/CdTe _{1.91nm} /MDMO-PPV/Au	0.34	300	0.301	3.1

1.7 Current-Voltage Characteristics of CdTe Multilayers

Photovoltaic devices are prepared with different sized- CdTe QDs and PDADMAC multilayers. A plot of the current density versus voltage for the four devices is shown in Figure 1.9. The open-circuit voltages of the cells are in the range of 400 -500 mV. It is found that smaller domain sizes lead to slightly higher efficiency ⁷.

The PV cell performance parameters, V_{oc} , J_{sc} , FF and MP are shown in Table 3. Both V_{oc} and J_{sc} decrease slightly with increasing size of quantum dot.

In rainbow model, three different sized QDs are adsorbed. (ITO/TiO₂/MPA/(CdTe_{1.91nm}-PDADMAC)/(CdTe_{1.83nm}-PDADMAC)/ (CdTe_{1.74nm}-PDADMAC)/MDMO-PPV/Au). The results appear to show that the photocurrent arises from contributions from all three particle sizes. In any case, any further discussion on this issue would require measurements of the IPCE for this device.

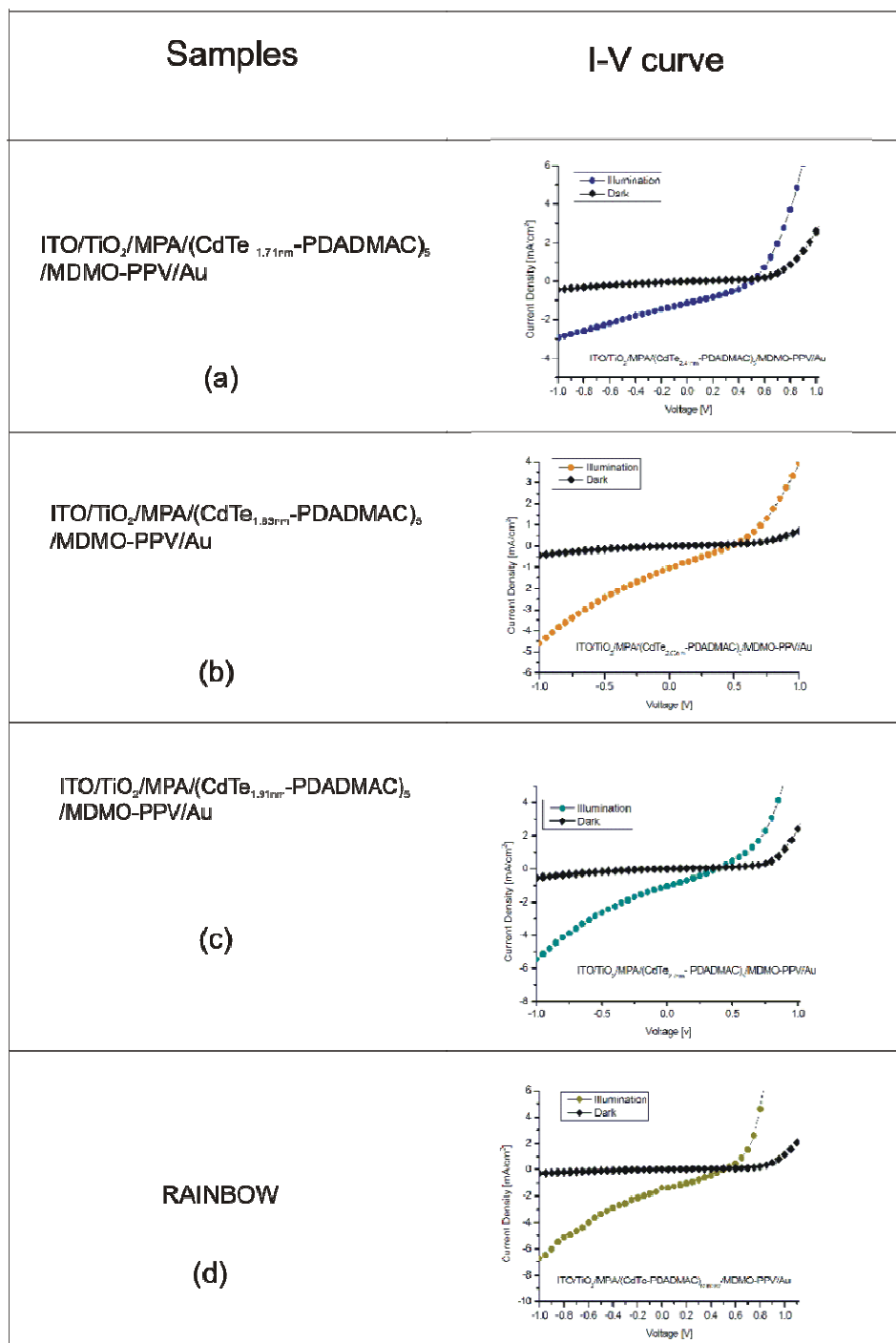


Figure 1.9 Current density vs Voltage(J-V) characteristics of solar cells with the structure of (a) ITO/TiO₂/MPA/(CdTe_{1.47nm} – PDADMAC)₅ /MDMO-PPV/Au (b) ITO/TiO₂/MPA/(CdTe_{1.83nm} – PDADMAC)₅ /MDMO-PPV/Au (c) ITO/TiO₂/MPA/(CdTe_{1.91nm} – PDADMAC)₅ /MDMO-PPV/Au (d) ITO/TiO₂/MPA/(CdTe – PDADMAC)_{3,RAINBOW} /MDMO-PPV/Au

Table 3. Measured performance characteristics of devices

Sample	J_{sc} (mA/cm ²)	V_{oc} (mV)	FF	MP(μW)
ITO/TiO ₂ /MPA/(CdTe _{1.74nm} -PDADMAC) ₅ /MDMO-PPV/Au	1.14	500	0.345	22
ITO/TiO ₂ /MPA/(CdTe _{1.83nm} -PDADMAC) ₅ /MDMO-PPV/Au	1.06	450	0.269	14
ITO/TiO ₂ /MPA/(CdTe _{1.91nm} -PDADMAC) ₅ /MDMO-PPV/Au	1.04	400	0.267	12
ITO/TiO ₂ /MPA/(CdTe-PDADMAC) _{rainbow,3} /MDMO-PPV/Au	1.37	500	0.345	26

1.8 Conclusion

It was also shown clearly that the colloidal CdTe QDs can be used as e sensitizer covering the visible range by controlling the size of the QD particles. Quantum size effects are anticipated to be a factor in QDs solar cell efficiency. Although the short circuit current measured from the QD-sensitized solar cell was smaller than those of the organic dye-cell, it was shown that the photocurrent can be increased by preparing multilayers of QDs . IPCE and overall conversion efficiencies achieved.

PART 2

2.1 Experimental

Ti –nanoxide (TiO₂) (Solaronix), Chlorophyllin coppered trisodium salt (Aldrich-Sigma) (CuChI) was purchased from the sources and used without purification.

Regioregular poly-3-hexylthiophene-2,5diyl (P3HT) was purchased from Rieke. P3HT is widely used as donor in organic solar cells. This material has higher hole mobility than any other known conjugated polymer until now, including poly (phenylvinylene)s. This high mobility is related to side-chain induced self-organization. Figure 2.1 shows the chemical structure of this used polymer.

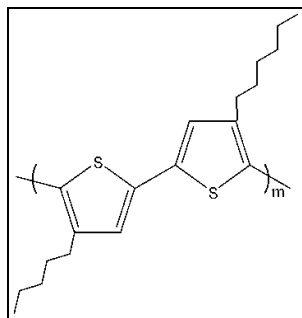


Figure 2.1. Chemical structure of poly(3-hexylthiophene)

2.2 Preparation of the Nanocrystalline TiO₂ Film Electrode

The nanocrystalline TiO₂ film was prepared by a similar procedure to that described in Chapter 6. Colloidal TiO₂ paste (Ti-Nanoxide T) was purchased from Solaronix. According to the supplier's specification, the particle size of TiO₂ is ca. 13 nm and the paste is well-suited for preparation of transparent photoelectrodes for dye-sensitized solar cells. Commercially available glass substrates covered with indium tin oxide (ITO, < 20 Ω cm⁻²) were used as transparent conducting substrates to prepare a TiO₂ photoelectrode. TiO₂ (Solaronix, T20) solution was spin-coated on the substrate. The electrodes were gradually heated till 450°C for 5h under ambient conditions to form a nanocrystalline TiO₂ film electrode.

2.3 Preparation of the Nanocrystalline TiO₂ Film Electrode Modified by a CuChl Adsorbed Layer

Copper chlorophyllin (CuChl) is produced on a large scale as a water-soluble dye for application in food coloring, cosmetics, and medicine. Sodium copper chlorophyllin is stabilized chlorophyll. Sodium copper chlorophyllin (Figure 2.2) is produced by replacing the magnesium atom with copper and sodium. Copper is introduced to make the dye more stable against photooxidation by reducing its excited-state lifetime.

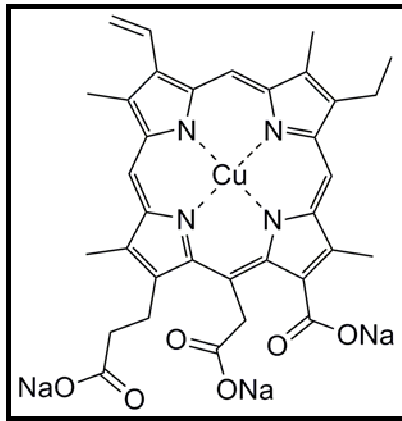


Figure 2.2. Chemical structure of Chlorophyllin sodium copper salt (CHPL)

An ITO glass plate with a nanocrystalline TiO_2 film was dipped into 70 mmol dm^{-3} CuChl in water solution at room temperature for 15 h. After dipping, the electrode was washed with copious amount of water, and then, the electrode was dried under vacuum overnight. The electrode became green after coating with CuChl dye molecules. Sensitized electrodes are denoted $(\text{ITO}/\text{TiO}_2/\text{CuChl})$.

2.4 Assembling the Solid State Dye Sensitized Solar Cell

P3HT (1wt %) in chlorobenzene was spincoated on $(\text{ITO}/\text{TiO}_2/\text{CuChl})$ modified electrode. Then 110 nm of gold was thermally evaporated onto $(\text{ITO}/\text{TiO}_2/\text{CuChl}/\text{P3HT})$. All investigated photovoltaic structures were fabricated in sandwich configurations $(\text{ITO}/\text{TiO}_2/\text{CuChl}/\text{P3HT}/\text{Au})$ (Figure 2.3).

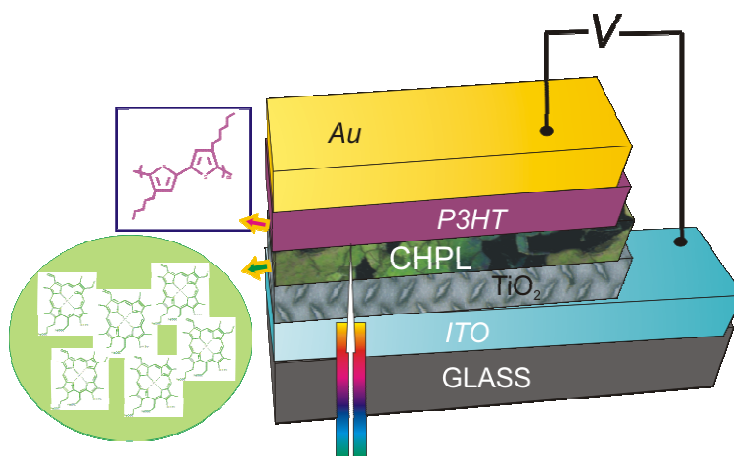


Figure 2.3. Device structure of studied solar cells

2.5 Experimental Setup

UV-Vis spectra were recorded in a 1 cm path length quartz cell on a Cary 100 Bio spectrophotometer. Atomic force microscope (AFM) measurements were done with a Dimension 3100 instrument from Digital Instruments (Santa Barbara, CA) in tapping mode. The details of photocurrent action spectra and photovoltaic properties of (ITO/TiO₂/CuChl/P3HT/Au) measurements were given in Part 1.

2. Results

2.7 UV-vis Absorption Spectrum of Used Materials in Solution and CHPL Layer onto a Nanocrystalline TiO₂ Film

UV-vis absorption spectra of CuChl adsorbed on a nanocrystalline TiO₂ film (ITO/TiO₂/CuChl) (Figure 8.4.a), a nanocrystalline TiO₂ electrode (ITO/TiO₂) (Figure 2.4.b), (ITO/TiO₂/P3HT) (Figure 2.4.c) and dilute CuChl solution (Figure 2.4.d) has been measured and shown Figure 8.4. CuChl solution is characterized by the sharp absorption bands in the Soret (390 nm) and in the Q-band region (625 nm)¹⁰.

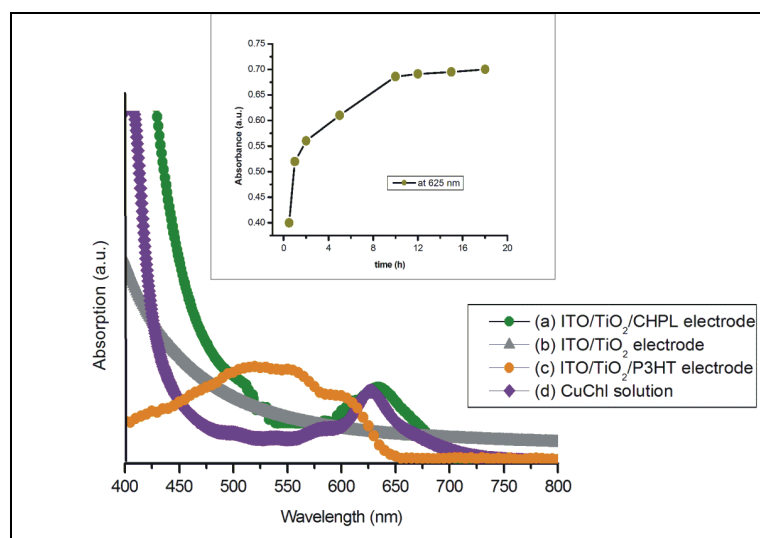


Figure 2.4. UV-vis absorption spectra of CuChl adsorbed on a nanocrystalline TiO₂ film (ITO/TiO₂/CuChl) (Figure 2.4.a), a nanocrystalline TiO₂ electrode (ITO/TiO₂) (Figure 2.4.b), (ITO/TiO₂/P3HT) (Figure 2.4.c) and dilute CuChl solution (Figure 2.4.d)

The (ITO/TiO₂/CuChl)(Figure 2.4.a), electrode displaces the characteristic absorption of CuChl with a maximum in the visible region at around 625 nm, indicating that the sensitization of TiO₂, electrode with dye molecules could extend the absorbance of the electrode into the visible region. The Q-bands of CuChl red-shift by 5 nm and broadened compared to the dye in water solution (Figure

(2.4.d), indicating a strong interaction between the dyes and the semiconductor surface¹¹. Figure 2.4.b is the absorption spectrum of a bare TiO₂ film. The bare TiO₂ film exhibits the fundamental absorption edge of anatase (350nm) in the UV region¹². Figure 2.4.c shows the absorption spectrum of (ITO/TiO₂/P3HT). It is seen that thin films of the chosen materials absorb visible light with a remarkable efficiency but that one semiconductor CuChl covers only some part of the visible region. This double layer cells containing two organic compounds such as P3HT and CuChl with their high absorption coefficient can absorb most parts of the visible solar radiation¹³.

The inset in Figure 2.4 shows change in the absorbance of excitonic peak at 625nm with adsorption time of CuChl on ITO/TiO₂ electrode. With increase of time, the absorbance increases more quickly in the early stage, slows down gradually, and then reaches an almost constant value. The higher increment of absorbance in the early adsorption time is attributed to the higher surface area of the mesoporous matrix available for absorption.

2.8 Morphology of Films

The surface morphology of ITO/TiO₂/CuChl modified surface was investigated using atomic force microscopy (AFM), and the results are shown in Figure 2.5. The TiO₂ film is microporous and these pores has a important function that the dye molecules can penetrate into electrode. After incorporation the CuChl, there is no change in the morphology of TiO₂ layer.

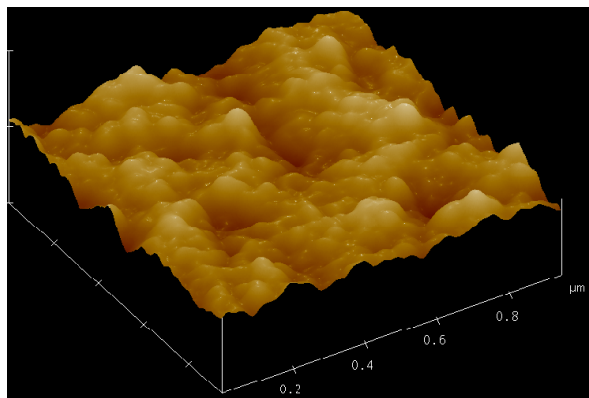


Figure 2.5 AFM images of ITO/TiO₂/CuChl modified electrode (size: 1μm x 1μm)

2.9 Photocurrent-Photovoltage Characterization of the Nanocrystalline TiO₂ Film Electrode Modified by CuChl and P3HT

Figure 2.6 shows the photocurrent–photovoltage characteristics of the sandwich solar cell based on the ITO/TiO₂/CuChl/P3HT/Au electrode irradiated with 100 mW cm⁻². The short-circuit photocurrent (I_{sc}) was 0.42 mA cm⁻² and the open-circuit photovoltage (V_{oc}) was 300 mV. The maximum power was

estimated to be $4.5 \mu\text{W}$ and the fill factor (FF) was estimated to be 32.1%. Liu et al.¹⁴ previously reported the photovoltaic conversion system using the ITO/TiO₂ film electrode modified by MgChl-*a*. In this report, the I_{SC} , V_{OC} , maximum power, and FF of a solar cell were $11 \mu\text{A cm}^{-2}$, 460 mV and $0.87 \mu\text{W}$ respectively. Thus, CuChl and P3HT anchored on nanocrystalline TiO₂ film is an efficient uv-visible and near-IR sensitization for a photovoltaic injection cell based on the nanocrystalline TiO₂ film electrode.

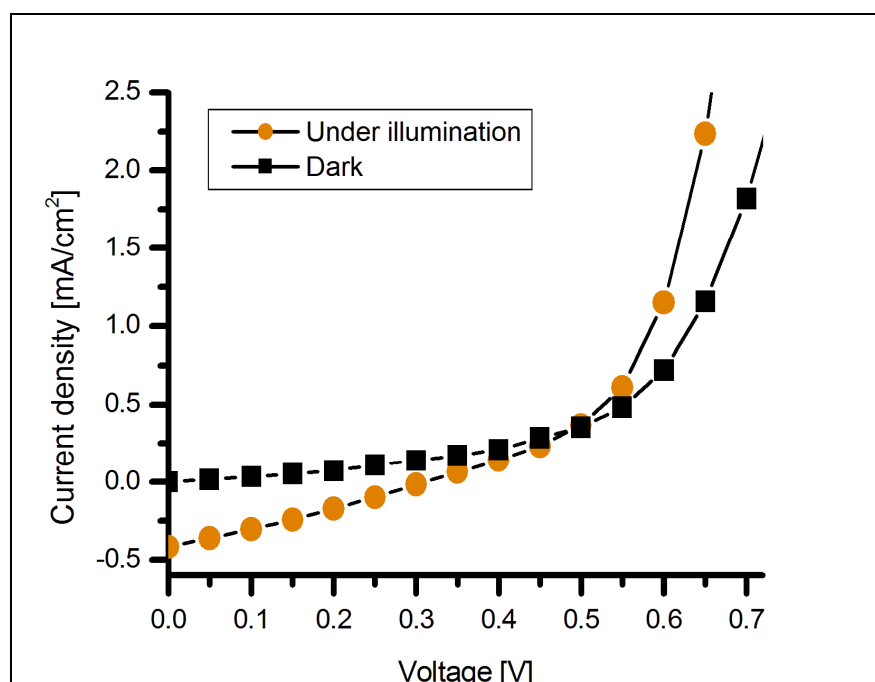


Figure 2.6. Photovoltage-photocurrent curve of the ITO/TiO₂/CuChl/P3HT/Au electrode

2.10 Photocurrent action spectrum of CuChl and P3HT modified TiO₂ Electrode

Figure 2.7 shows a comparison of the incident photon to current efficiency (IPCE) of the hybrid device with CuChl and P3HT with the absorption spectra (inset in Figure 2.7). The %IPCE is the percentage of electrons, measured under short circuit current conditions, related to the number of incident photons and is used to obtain information on the number of photons of different energy that contributes to the charge generation in the solar cell. The comparison of the IPCE and the optical absorption spectra gives information on the charge carrier generation mechanism. As can be seen from this figure both CHPL and P3HT contribute to the charge carrier generation¹⁵.

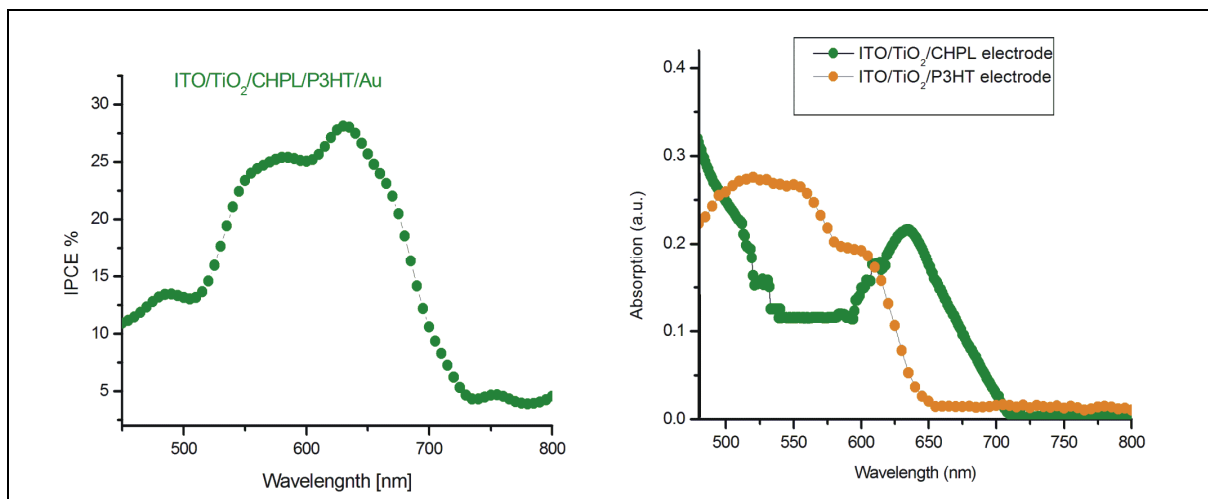


Figure 2.7 Photocurrent action spectra of ITO/TiO₂/CuChl/P3HT/Au electrode, (a) absorption spectra of CuChl adsorbed on a nanocrystalline TiO₂ film (ITO/TiO₂/CuChl) (b) (ITO/TiO₂/P3HT)

The photocurrent response curve at longer wavelength should be resulted from contribution of the P3HT due to its absorption between 470 and 600 nm. This finding demonstrates that photo-generated excitons should be created in both the CuChl and P3HT layers according to the photocurrent response curve.

2.11 Conclusion

In this work CuChl with carboxyl groups and P3HT adsorbed on a nanocrystalline TiO₂ film electrode were prepared and the photoelectrical properties of the solar cell using visible light sensitization of a nanocrystalline TiO₂ film by CHPL and P3HT was investigated. The efficient light harvesting in plants was successfully imitated by adsorbing monolayers of the chlorophyll derivative on nanostructured TiO₂ films. In conclusion, the photovoltaic conversion device based on the UV-visible and near-IR sensitization of CuChl and P3HT was developed.

2.12 Scientific Contributions Resulting from Exchange Grant

- 7th Swiss Snow Symposium, February 2009, Lenk, Switzerland

Seminar Title: “Novel Photoactive Systems Involving Semiconductor Quantum Dots”

- EMPA PhD Students Symposium, November 2008, St. Gallen, Switzerland

Poster Title: “Photosensitization of TiO₂ Solar Cell with Chlorophyll Salt”

2.13 References

- (1) Anders Hagfeldt; Gratzel, M. *Acc. Chem. Res* **2000**, *33*, 269-277.
- (2) Mette, H. *Z. Physik* **1953**, *134*, 566.
- (3) Lee, Y.-L.; Huang, B.-M.; Chien, H.-T. *Chemistry of Materials* **0**, *0*.
- (4) Robel, I.; Subramanian, V.; Kuno, M.; Kamat, P. V. *J. Am. Chem. Soc.* **2006**, *128*, 2385-2393.
- (5) Laurence M. Peter, D. J. R., Elizabeth J. Tull and K. G. Upul Wijayantha. *Chem. Commun.*, **2002**, 1030-1031.
- (6) Hyo Joong Lee, D.-Y. K., Jung-Suk Yoo, Jiwon Bang, Sungjee Kim, and Su-Moon Park. *Bull. Korean Chem. Soc.* **2007**, *28*, 953.
- (7) Robel, I.; Kuno, M.; Kamat, P. V. *J. Am. Chem. Soc.* **2007**, *129*, 4136-4137.
- (8) Hyo Joong Lee, J.-H. Y., Henry C. Leventis, Shaik M. Zakeeruddin, Saif A. Haque,; Peter Chen, S. I. S., Michael Gratzel, and Md. K. Nazeeruddin. *J. Phys. Chem. C* **2008**, *112*, 11600–11608.
- (9) Gebeyehu, D.; Brabec, C. J.; Padinger, F.; Fromherz, T.; Hummelen, J. C.; Badt, D.; Schindler, H.; Sariciftci, N. S. *Synthetic Metals* **2001**, *118*, 1-9.
- (10) Schlettwein, D.; Oekermann, T.; Yoshida, T.; Tochimoto, M.; Minoura, H. *Journal of Electroanalytical Chemistry* **2000**, *481*, 42-51.
- (11) Kamat, P. V. *Chemical Reviews* **1993**, *93*, 267-300.
- (12) Tang, H.; Lévy, F.; Berger, H.; Schmid, P. E. *Phys. Rev. B J1 - PRB* **1995**, *52*, 7771 LP - 7774.
- (13) Sariciftci, H. H. a. N. S. *J. Mater. Res.* **2004**, *19*, 1924.
- (14) Bao-Qi Liu, X.-P. Z., Wei Luo. *Dyes and Pigments* **2008**, *76*, 327-331.
- (15) Serap Gunes, N. M., Jovan M Nedeljkovic and; Sariciftci, N. S. *Nanotechnology* **2008**, *19*, 424009.

Acknowledgements

The author is thankful to the European Science Foundation-Organisolar for this grant. The colleagues in Linz, especially Dr.Elif Arici-Bogner, Robert Koeppel and Martin Egginger, are acknowledged for their help, the valuable discussions and their friendly atmosphere.